JAST, Vol. 3, No. 1, pp 51–60

JAST
Journal of Aerospace Science and Technology

Research Note

LES Numerical Study of Reynolds Number Effects on Flow over a Wall-Mounted Cube in a Channel

M. Farhadi[1], K. Sedighi[2]

Turbulent flow over wall-mounted cube in a channel was investigated numerically using Large Eddy Simulation. The Selective Structure Function model was used to determine eddy viscosity that appeared in the subgrid scale stress terms in momentum equations. Studies were carried out for the flows with Reynolds number ranging from 1000 to 40000. To evaluate the computational results, data was compared with experimental results at Re=40000, showing a good correspondence. In this study the effect of Reynolds numbers on flow characteristics such as time-averaged streamlines, turbulent intensity and Reynolds stresses were investigated. Results of computations show that the flow with higher Reynolds number has a shorter reattachment length and by increasing the Reynolds number, the number of horseshoe vortex in the upstream decreases. The vortex structures were similar in the upstream of the cube for time-averaged and instantaneous flow field. While on the downstream, the vortex structure does not show any similarity and had a complex flow field structure. Reynolds stress became stronger at the sides of the cube where the horseshoe vortexes were built, and gained more importance at the higher Reynolds number.

NOMENCLATURE

C_k	Kolmogorov constant
$E(K)$	Kinetic energy spectrum
$G_{\Delta x}(x_i)$	Filter function
H	Square cylinder height
K_c	Cut-off wavenumber
P	Pressure
Re	Reynolds number based on the height of the square cylinder, U_{mean} H/υ
t	Time step
U_c	Convective mean velocity
u_i	Instantaneous velocity components
u	Velocity vector
U_{mean}	Mean Velocity at the entrance
x_i	Cartesian coordinate, x_1, x_2, x_3
x	Position vector

Greek Symbols

α	Angle
Δ	Minimum grid spacing
Δx_i	Grid spacing
Φ_{20°	Indicating function, equation (8)
υ_t^{SF}	Turbulent eddy-viscosity obtained from SF
υ	Kinematic viscosity
τ_{ij}	Subgrid scale (SGS) stress tensor

1. *Faculty of Mechanical Eng. of Mazandaran Univ., Babol, Iran. P. O. Box: 484, E-mail: mfarhadi@nit.ac.ir /m.farhadi@umz.ac.ir*
2. *Faculty of Mechanical Eng. of Mazandaran Univ., Babol, Iran. P. O. Box: 484.*

INTRODUCTION

Turbulent flow around bluff bodies has attracted increasing attention not only for its academic aspects but also for its practical importance. Flow passing a wall-mounted cube has a wide range of engineering applications, such as air-cooling of the electronic boards and the study of flow around tall buildings. In

practice there is a great need to predict such flows and the loading imposed on the bodies. However, this is a difficult task even for relatively simple geometries. Flow separation and reattachment, unsteady vortex shedding and large-scale turbulence structures are among the important phenomena observed in such flow configurations.

There is vast literature concerning experiments done on this geometry [1-6]. The majority of works are by Martinuzzi and Tropea [5], and Hussein and Martinuzzi [6] for Reynolds number of 40000. They investigated a three-dimensional flow around surface-mounted cubes in a channel experimentally for Reynolds number of 40000. Their flow patterns show the very complex flow nature in spite of its simple geometry. To predict turbulent flow behavior over a wall-mounted cube in a channel, various numerical approaches have been proposed. One of them is Large Eddy Simulation (LES) which tries to simulate the largest scales of motion while treating the small scales by model. It would be appropriate for the flow over a cube to be treated by LES, as there are large vortices generated in such a flow. Many researchers have studied this flow filed with different LES models. Shah and Ferziger [7] were among the pioneers in doing LES of flow over a surface mounted cube at Reynolds number 40000, in good correspondence with the experiment. This geometry was investigated in the Rottach-Egren [8] workshop, and recently by Krajnovic and Davidson [9, 10], Rahnama and Farhadi [11] and Farhadi and Rahnama [12] at Reynolds number 40000 with different LES models. Their results showed that LES models are capable of this flow field with acceptable accuracy even for coarse grid points (Ref. [10, 12]). It must be mentioned that the computational cost of LES approach is higher than the other methods like RANS. Recently, Hwang and Yang [13] studied the vortical structures of flow around a wall-mounted cube in a channel at low to moderate Reynolds numbers up to 3500 using Direct Numerical simulation (DNS). Their results showed that as the Reynolds number increases, the structure of the horseshoe vortex system becomes more complex, and the number of vortices increases in pairs. In the case of a turbulent wake, however, it was observed that the flow becomes less coherent in the near-wall region downstream of the obstacle. Instead, coherent structures such as lateral and hairpin vortices are found present in the vicinity of the two lateral faces of the cube and in the turbulent near-wake region, respectively.

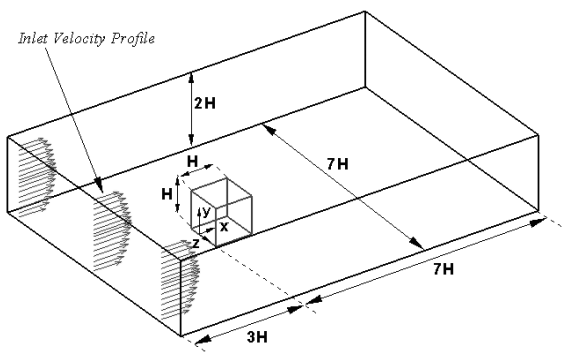

Figure 1. Geometry of problem

In this study, the flow over a wall-mounted cube in a channel was investigated by Selective Structure Function (SSF) model from LES models. The Effects of Reynolds number on flow over wall-mounted cubes were investigated at moderate to high Reynolds numbers, hence forth has not been studied yet. Characteristics of flow field including time-averaged and instantaneous streamlines, contours of vorticity and turbulent properties were evaluated.

MATHEMATICAL MODEL

In LES approaches, larger scale three-dimensional unsteady turbulent motions are directly presented, whereas the effect of small scales of motion is modeled. To do this, a filtering operation is introduced to decompose the velocity vector (u_i) into the sum of a filtered (or resolved) component, $\bar{u}$ and a residual (or subgrid-scale) component (u'). This operation can be represented with a filter of width Δx such that convolution of any quantity $f(x_i, t)$ by the filter function $G_{\Delta x}(x_i)$ is in the form:

$$\bar{f}(x_i,t) = \int f(y_i,t) G_{\Delta x}(x_i - y_i) dy_i, \qquad f' = f - \bar{f} \quad (1)$$

The equations for evolution of the filtered velocity filed, are derived from the Navier-Stokes equations. These equations are of the standard form, with the momentum equation containing the residual stress tensor. Application of the filtering operation to the continuity and Navier-Stokes equations gives the resolved Navier-Stokes equations, which, in non-dimensional incompressible from, are:

$$\frac{\partial u_i}{\partial x_i} = 0, \quad (2)$$

$$\frac{\partial \bar{u}_i}{\partial t} + \frac{\partial}{\partial x_j}(\bar{u}_i \bar{u}_j) = -\frac{\partial \bar{P}}{\partial x_i} + \frac{1}{\mathrm{Re}} \nabla^2 \bar{u}_i - \frac{\partial \tau_{ij}}{\partial x_j}, \quad (3)$$

where $\bar{P}$ is the pressure, $\bar{u}_1$, $\bar{u}_2$ and $\bar{u}_3$ are the streamwise, cross-stream and spanwise component of velocity, respectively. These govern the dynamics of the large, energy-carrying scales of motion. Reynolds number is defined as U_{mean} H/v, where U_{mean} and H are the average velocity of entrance profile and cube height respectively. The effect of small scales upon the resolved part of turbulence appears in the subgrid scale (SGS) stress term, $\tau_{ij} = \overline{u_i u_j} - \bar{u}_i \bar{v}_j$, which must be modeled.

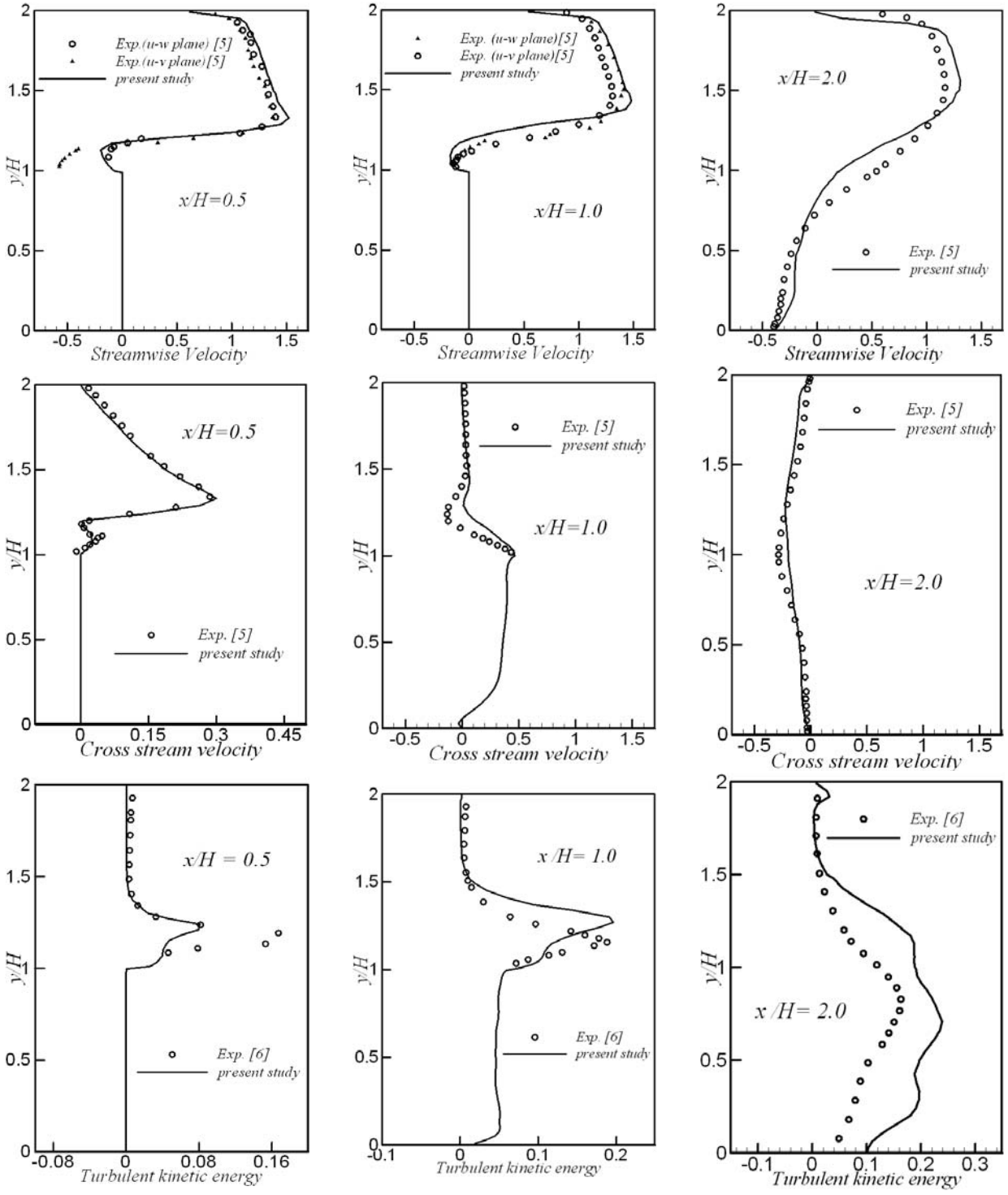

Figure 2. Time-averaged streamwise, cross stream velocity and turbulent kinetic energy profiles compared with experiment at the plane z=0 at Reynolds number 40000.

The main effect of the subgrid-scale stresses is dissipative around the cut-off spectrum, i.e., withdrawing energy from the part of the spectrum that can be resolved. One model for subgrid-scale stress term τ_{ij} is based on its dependence on filter strain rate through an eddy-viscosity:

$$\tau_{ij} = \upsilon_t(\frac{\partial \bar{u}_i}{\partial x_j} + \frac{\partial \bar{u}_j}{\partial x_i}) + \frac{1}{3}\tau_{kk}\delta_{ij}. \quad (4)$$

In this study, the eddy viscosity (υ_t) was evaluated

using subgrid-scale (SGS) model of Structure Function (SF) and Selective Structure Function (SSF) models. In the Structure Function model, the eddy viscosity is evaluated according to [14]:

$$v_t^{SF}(x,\Delta c,t) = 0.105 C_k^{-3/2} \Delta c \sqrt{F_2(x,\Delta c,t)}, \tag{5}$$

where $\Delta c = (\Delta x_1 \times \Delta x_2 \times \Delta x_3)^{\frac{1}{3}}$ is the geometric mean of the meshes in the three spatial directions. C_k is Kolmogrov constant and F_2 is the local structure function constructed with the filtered velocity field $\bar{u}(x,t)$:

$$F_2(x,\Delta c,t) = \frac{1}{6}\sum_{i=1}^{3} \Big\langle [\bar{u}(x,t) - \bar{u}(x+\Delta x_i,t)]^2 + [\bar{u}(x,t) - \bar{u}(x-\Delta x_i,t)]^2 \Big\rangle \left(\frac{\Delta c}{\Delta x_i}\right)^{2/3}. \tag{6}$$

F_2 was calculated with a local statistical average of square (filtered) velocity differences between x and the six closest points surrounding x on the computational grid. In some cases, the average may be taken over four points parallel to a given plane.

In the Selective version of the Structure Function model, the eddy viscosity was switched off in the regions where the flow is not three-dimensional enough. The three-dimensional criterion was as the following: one measures the angle (α) between the vorticity at a given grid point and the average vorticity at the six closest neighboring points (or the four closest points in the four-point formulation). If this angle was less than 20^o, the most probable value according to simulations of isotropic turbulence at the resolution of 32^3-64^3, the eddy viscosity would be cancelled and only molecular dissipation acts. In this situation the flow is locally close to a two-dimensional state. As compared to the original SF model, this subgrid-scale model dissipates the resolved scale energy at fewer points of the computational domain and the model constant of 0.105 (see equation (5)) has then to be increased to satisfy energy conservation. To correspond the model constant with the SF model, it was calculated by eddy viscosity requirement that has given by SSF model and averaged over the entire computational domain. The calculated model constant then multiplied by 1.56 [15].

$$v_t^{SSF}(x,\Delta c,t) = 0.1638 \Phi_{20^\circ}(x,t) C_K^{-3/2} \Delta c [F_2(x,\Delta c,t)]^{1/2}, \tag{7}$$

where $\Phi_{20^\circ}(x,t)$ is the indicating function based on the value of α):

$$\Phi_{20^\circ}(x,t) = \begin{cases} 1 & \text{if } \alpha \geq 20^\circ \\ 0 & \text{if } \alpha < 20^\circ \end{cases} \tag{8}$$

Farhadi and Rahnama [12] showed a smooth varying function rather than an abrupt cut-off. This can predict the distribution of energy between small and large eddies better than the standard form of this function, so $\Phi'_{20^\circ}(x,t)$ used instead of $\Phi_{20^\circ}(x,t)$ which is defined as:

$$\Phi'_{20^\circ}(x,t) = \begin{cases} 0 & \text{for } \alpha < 10^\circ \\ e^{-\left(\frac{d\alpha}{3^\circ}\right)^2} & \text{for } 20^\circ \geq \alpha \geq 10^\circ \text{ and } d\alpha = |\alpha - 20^\circ| \\ 1 & \text{for } \alpha > 20^\circ \end{cases} \tag{9}$$

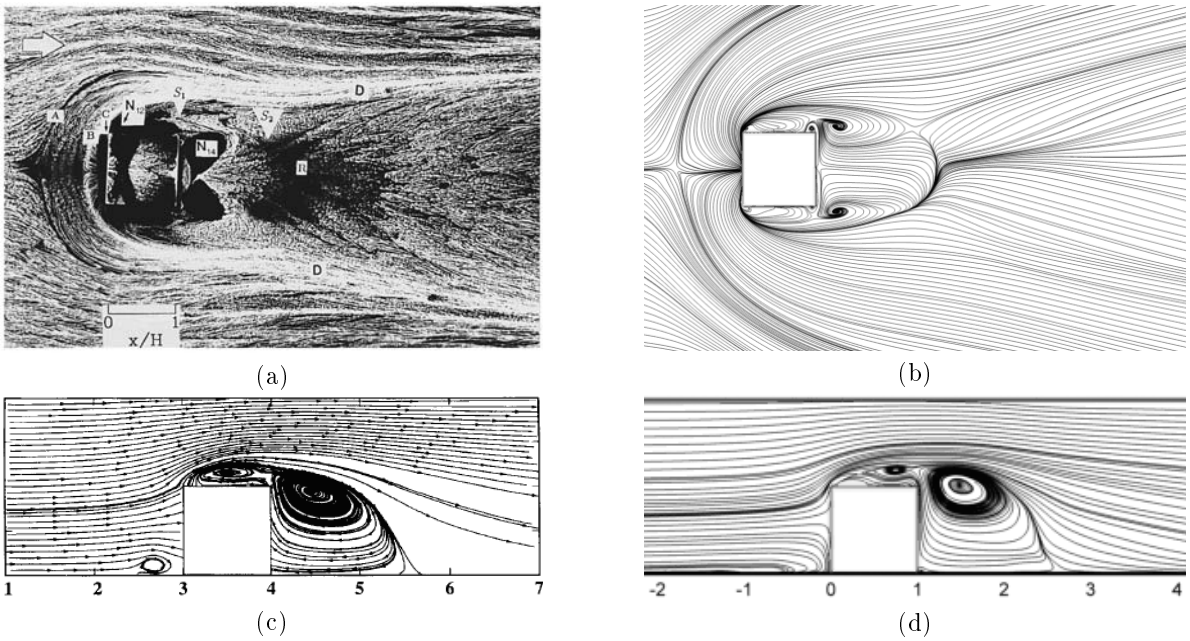

Figure 3. Time-averaged streamlines at the floor of the channel ((a) Reference [5] and (b) present study) and centerline of the cube ((c) Reference [5] and (d) present study) at Reynolds number 40000.

NUMERICAL METHOD AND COMPUTATIONAL DOMAIN

The governing equations presented in the preceding section were discretized using a finite volume method with a staggered grid. The convective terms were discretized using the QUICK scheme. The convective and diffusive fluxes appearing in the momentum equations were treated explicitly in the present computations. A third order Runge-Kutta algorithm was used for the time integration in conjunction with the classical correction method at each sub-step. The continuity equation (1) and the pressure gradient term in the momentum equation (2) were treated implicitly, while the convective and diffusive terms are treated explicitly. This method, called semi-implicit fractional step method, provides an approach that does not use pressure in the predictor step as in the pressure corrector method (such as the well-known SIMPLE family of algorithms). The linear system of pressure is solved by an efficient conjugate gradient method with preconditioning. The computational domain consists of a plane channel with a cubic obstacle of dimension (H) mounted on one of its walls (Figure 1).

Channel height was selected as 2H and the spanwise width of the channel was selected as 7H such that the

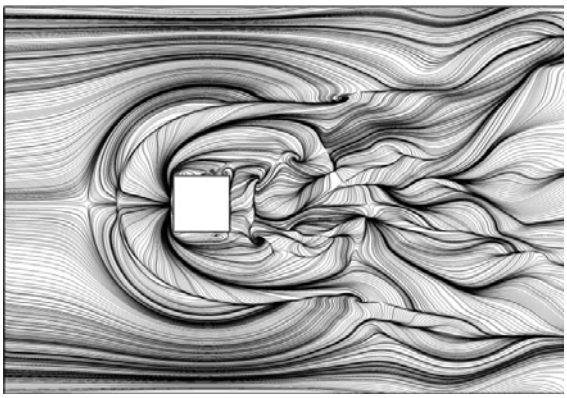

Figure 5. Time-averaged streamlines at the floor of the channel at Reynolds number 3200.

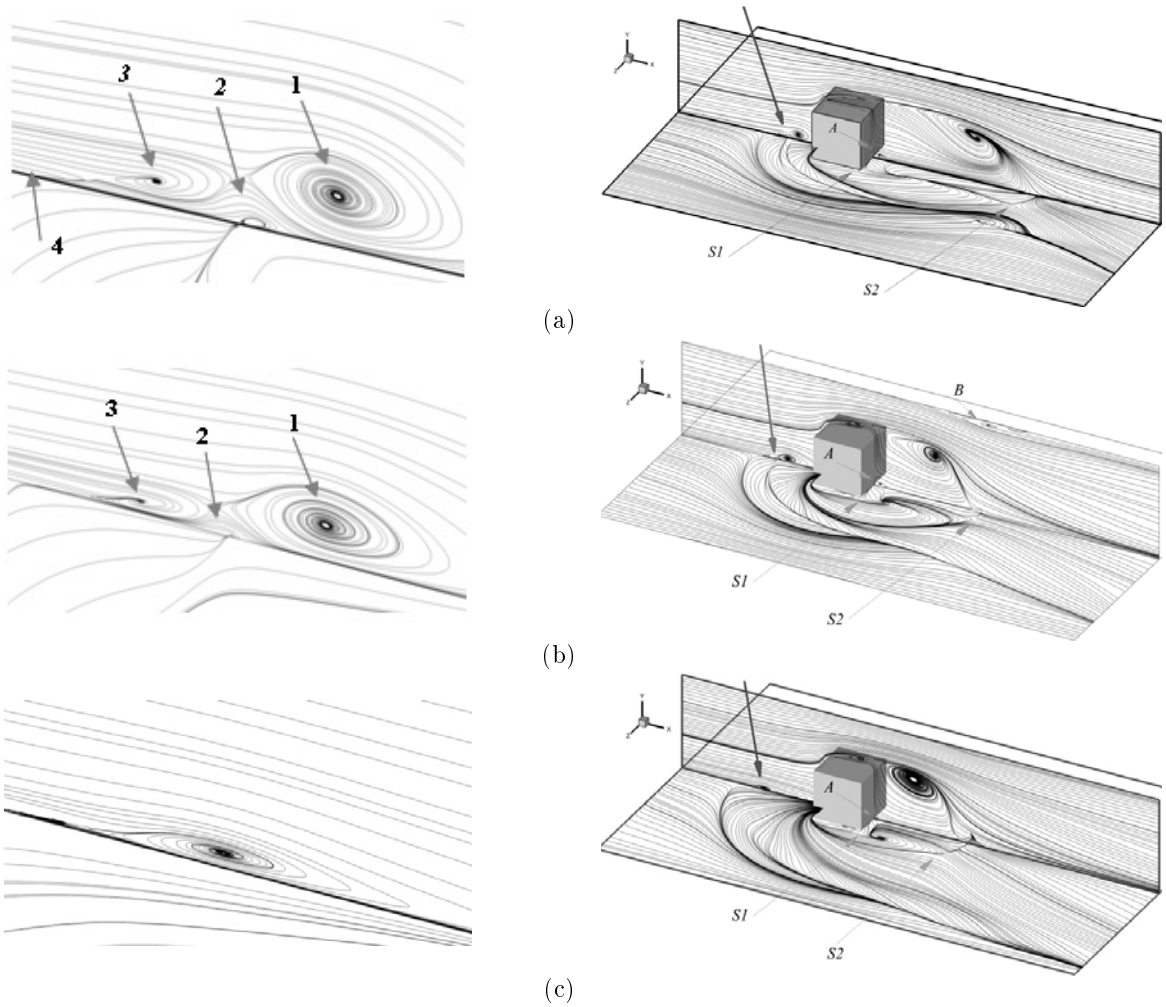

Figure 4. Time-averaged streamlines at the floor and centerline of the channel at Reynolds number (a) 1000, (b) 3200 and (c) 10000.

cube is located in the middle with equal distance from the spanwise boundaries of 3H. The upstream distance from the front side of the cube to the inlet boundary was selected as 3H and the downstream distance was 6H. The inlet boundary condition was selected as a fully developed turbulent velocity distribution (one-seventh power law). The outlet boundary condition is of convective type with U_c equalling to mean velocity as follows:

$$\frac{\partial u_1}{\partial t} + U_C \frac{\partial u_1}{\partial x_1} = 0. \tag{10}$$

Obviously, such convective boundary condition is capable of predicting unsteady flow behavior at the exit with good accuracy [8]. The spanwise boundary condition was selected as periodic. The minimum grid spacing used in the present computations is 0.03 in all directions adjacent to the cube surface with a grid expansion ratio of 1.05, and the no-slip boundary condition was used at the wall of cube and channel. The number of grid points used in the present computation, was $113\times51\times100$ in the x-, y- and z-direction, respectively. The CFL (Courant-Friedrichs-Lewy) number is less than one for all computations with a maximum value of 0.95. The average time in the simulation was $200H/U_{mean}$ where H is the cube height and U_{mean} is the bulk velocity at the inlet. In this study the Reynolds number was selected ranging from 1000 to 40000.

RESULTS

Results are represented in two parts: In the first part, the accuracy of the solution method was investigated by comparing the results of the computational data with the measurements of Martinuzzi and Tropea [5] and Hussein and Martinuzzi [6] at Reynolds number 40000. In the second part, the effect of Reynolds number on the flow over a wall-mounted cube in the channel was evaluated.

Validation

Results of LES computations for flow over a wall-mounted cube can be represented in the form of time-averaged quantities for which experimental data is available. Figure 2 shows the time-averaged streamwise, cross stream velocity and turbulent kinetic energy profiles in different positions at the plane z=0 compared with the experiment. It is observed that the results of the computational data show good accuracy especially for streamwise and cross steam velocity profiles. It should be mentioned that although some discrepancies exist at the turbulent kinetic energy profiles, the numerical data follow the trend of experiment. Probability is due to the use of the coarse grid resolution near the wall. In this area, energy is transfered from large to small scale eddies that capable of using fine grid resolution in this region. Furthermore, the difference between numerical and experimental data in the length and form of the recirculation zones may have created such discrepancies.

The turbulent flow over a wall-mounted cube in

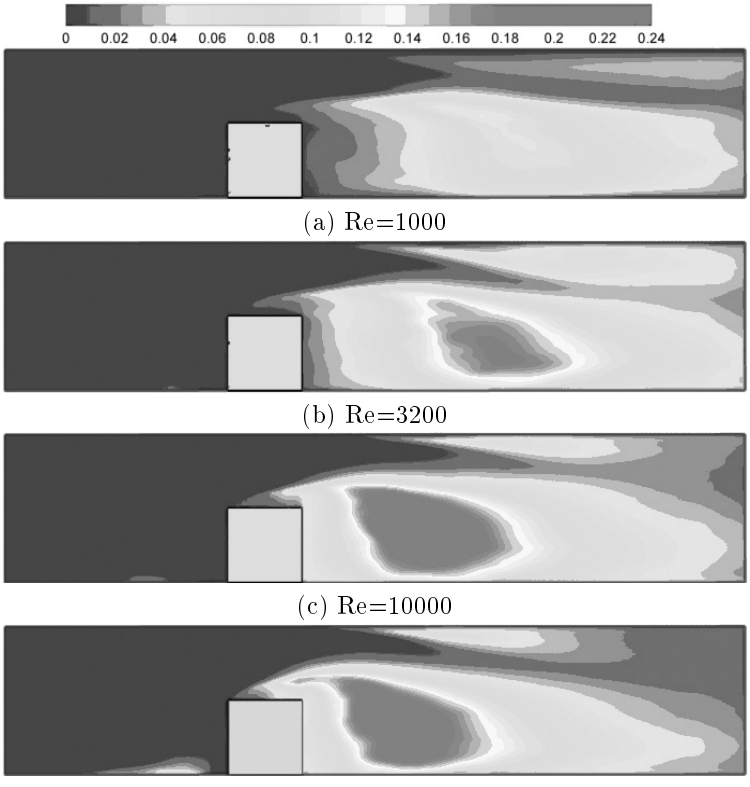

(a) Re=1000

(b) Re=3200

(c) Re=10000

(d) Re=40000

Figure 6. Time-averaged contours of turbulent kinetic energy at the centerline of the cube for different Reynolds numbers.

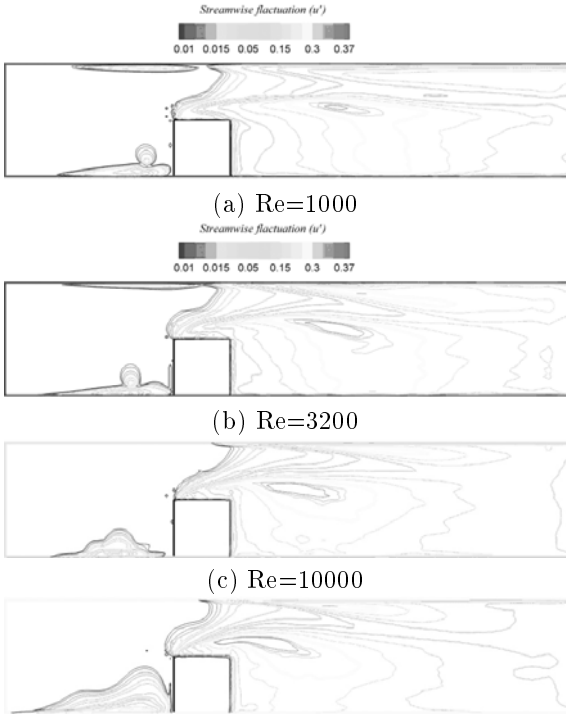

(a) Re=1000

(b) Re=3200

(c) Re=10000

(d) Re=40000

Figure 7. Time-averaged streamwise velocity fluctuation at the center line of the channel at different Reynolds numbers.

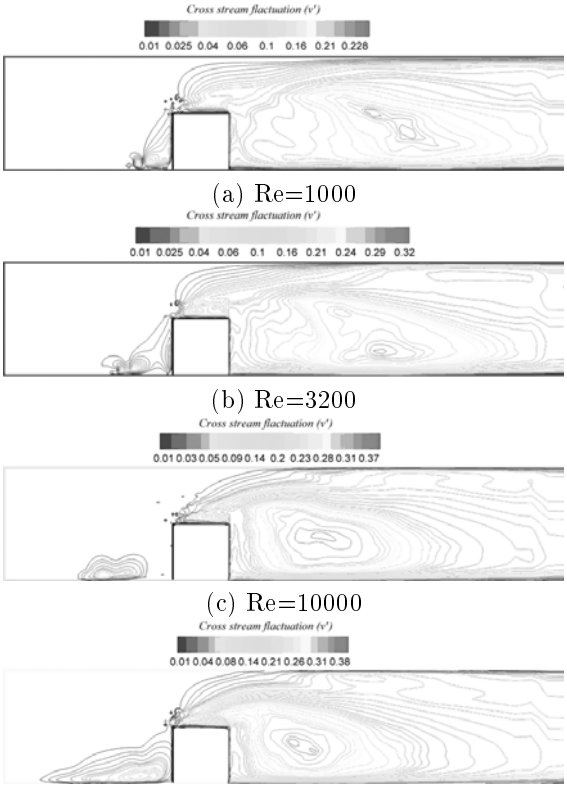

(a) Re=1000

(b) Re=3200

(c) Re=10000

(d) Re=40000

Figure 8. Time-averaged cross stream velocity fluctuation at the center line of the channel at different Reynolds numbers.

a channel has a very complex structure, such as hours shoe vortex and recirculation zones. Figure 3(a) and 3(c) show the oil visualization of flow field over the cube and streamlines at the floor and centerline of the channel respectively which was reported by Martinuzzi and Tropea [5]. The numerical results follow the trend of experiment with some discrepancy. The reattachment lengths were predicted well (0.9 and 1.601) compared to measurement (1.04 and 1.61 Reference [5]) in the upstream and downstream of the cube respectively. It should be mentioned that the computational data could not show the converging –diverging form of flow field in the floor of the channel which was observed from oil visualization by Ref. [5 and 6]. It is observed that the second saddle point was predicted at the downstream of the cube which was shown by arrow in the Figure 3(b).

Flow field

Figure 4 shows time-averaged streamlines at the floor and centerline of the channel for different Reynolds number (1000, 3200 and 10000). It is observed that there are several recirculation regions in the upstream, downstream and top of the cube for all Reynolds numbers. In the upstream of the cube, three recirculation regions are seen clearly for Reynolds number 1000 and 3200. The fourth small vortex region is cleaved to the wall toward the entrance of the channel, which is only observed at Reynolds number 1000. It should be mentioned that those vortex regions were reported by Hwang and Yang [13]. By increasing the Reynolds number, the structure and number of vortexes were changed. The second vortex was omitted and the first and third vortex changed to the vortex which was observed at Reynolds number 10000 and higher.

There are two recirculation regions in the downstream of the cube. The primary recirculation zone begins from the leading edge of the cube. The wake circulates over a larger area in the downstream. The secondary is very small and is situated at the rear side of the cube, below the primary vortex core (point A). The length of these recirculation regions decreases by increasing the Reynolds number and shifts the center of vortex core to the leading edge of the cube. In the lateral sides of the cube, there are two saddle points, observed in experiment in Reference [5] (Figure 3(a), points S_1 and S_2) which are separated by a distance. The results of the computational data show these saddle points for all Reynolds numbers. Another recirculation region appeared downstream of the cube attached to the upper wall of the channel (point B), as observed in Figure 4(b) at Reynolds number 3200. It should be mentioned that the existence of these small recirculation zones was also reported by authors in [8] and [16].

Figure 5 shows instantaneous streamlines at the floor of the channel for Reynolds number 3200. It is shown that the flow field in the upstream is the same as time-averaged results, while the structure of the flow field is very complex and different in the downstream. Figure 6 shows variation of time-averaged contours of turbulent kinetic energy for different Reynolds number at the centerline of the cube (plane z=0). It is observed that the maximum turbulent

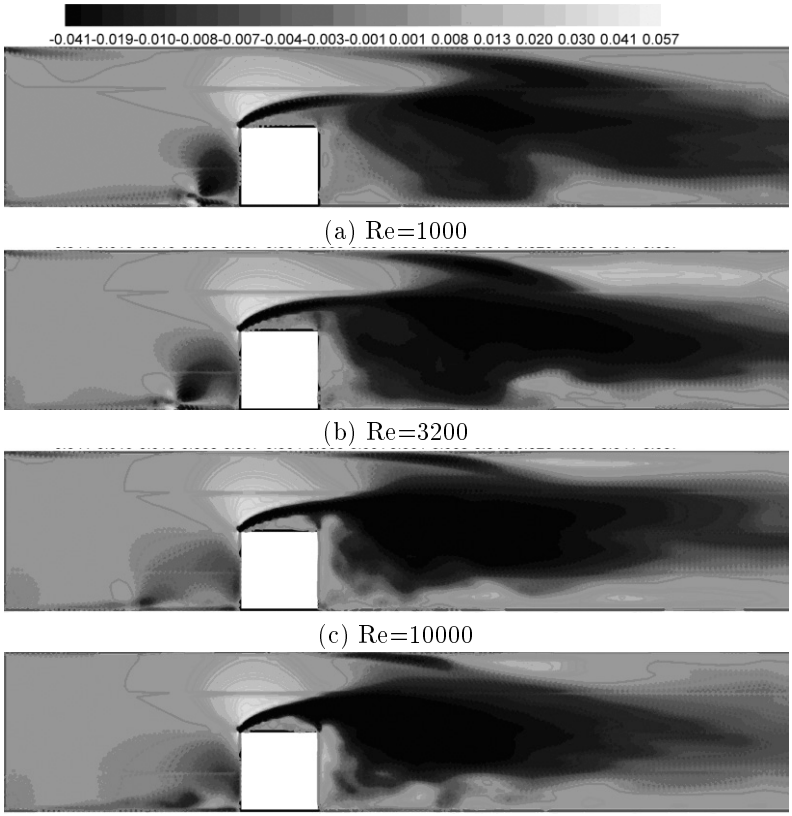

(a) Re=1000

(b) Re=3200

(c) Re=10000

(d) Re=40000

Figure 9. Time-averaged contours of magnitude of Reynolds stress ($u'v'$) at the center line of the channel at different Reynolds numbers.

Table 1. Reattachment lengths in the upstream and downstream of the cube for different Reynolds numbers.

Reynolds number	Recirculation length (upstream)	Recirculation length (downstream)
1000	1.071	3.83
3200	1.17	2.12
10000	1.15	1.9
40000	0.9	1.601
40000, Experimental [5]	1.04	1.61
40000, Experimental [6]	1.04-0.95	1.67

intensity was at the center of the recirculation zone in the downstream of the cube. This caused maximum velocity at the center of the vortex core. By increasing the Reynolds number, the recirculation center move towards the rear of the cube so that the maximum intensity of the turbulence shifts to the wall of the cube. It should be mentioned that the maximum quantity of the turbulent kinetic energy increases with increasing the Reynolds number.

Time-averaged streamwise and cross stream fluctuations (u' and v') were shown in Figures 7 and 8 at the centerline of the channel for different Reynolds numbers. The maximum velocity fluctuations occur in the vortex region. The maximum value of u' occurs in the center of vortex due to the highest streamwise velocity in this point. On the other hand, the maximum value of cross stream velocity (v') occurs in the lower level of vortex core position, which the flow has of higher upward acceleration. This can be observed clearly in Figures 7 and 8. It can also be seen as the Reynolds number increases, with the maximum values of the u' and v' moving toward the cube. This is because of the movement of the vortex core toward the obstacle.

Stresses fluctuated between negative and positive values depending on the vortex structure around the wall-mounted obstacle. Figure 9 shows time-averaged contours of magnitude of Reynolds stress ($u'v'$) at the centerline of the channel for different Reynolds numbers. Hence, there was a small positive value immediately behind the obstacle due to the small corner vortex. Values became strongly negative within the recirculation region and more strongly positive as the flow reattached and recovered. This phenomenon has been observed in other studies of flow over wall-mounted obstacle [17].The LES was able to detect

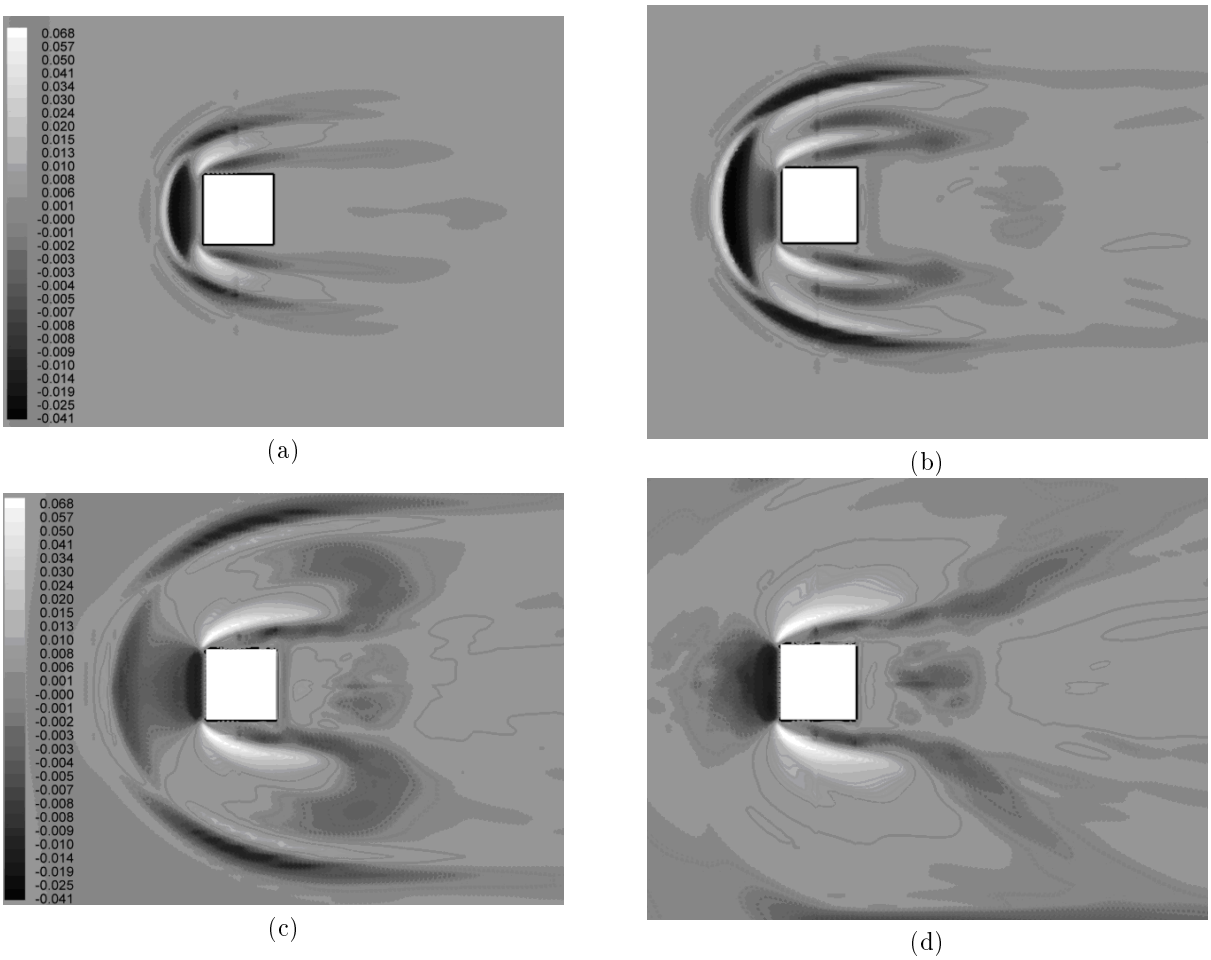

Figure 10. Time-averaged contours of magnitude of Reynolds stress ($u'v'$) at the floor of the channel at different Reynolds numbers.

the presence of favorable and adverse pressure gradients at the wall as the flow expanded and contracted over the obstacle. A steady-state numerical method would not resolve these aspects of the flow, leading to inaccuracies in the estimation of recirculation zone statistics and the effect of the bed-mounted obstacle on downstream flow mixing and instantaneous bed forces [17].

Figure 10 shows the time-averaged Reynolds stress contours at the floor of the channel for different Reynolds numbers. It is observed that the blockage effect of the obstacle creates an adverse pressure gradient which causes the flow to separate and trail off along the obstacle, forming a horseshoe vortex. We can identify a horseshoe-shaped region of strong shear stress around the obstacle, whose magnitude is approximately several times larger than its surrounding. As the Reynolds number increases, the number of horseshoe vortex decreases. Thus, it can be observed that the maximum value of $u'v'$ only occurs at the sides of the cube.

Table 1 shows characteristics of flow over a wall-mounted cube in a channel for different Reynolds numbers. It is observed that the results of the present work at Reynolds number 40000 shows good accuracy compared with the experimental data of Martinuzzi and Tropea [5] and Hussein and Martinuzzi [6]. It should be mentioned that the variation of the reattachment lengths in the upstream and downstream of the cube is not very significant, except for Reynolds number 1000. These results show that the overall behavior of flow field is nearly constant for Reynolds number 3200 to 40000.

CONCLUSION

Turbulent flow over a wall-mounted cube was investigated for different Reynolds numbers by Large Eddy Simulation. Studies were carried out for the flows with Reynolds number ranging from 1000 to 40000. To evaluate the computation results, data was compared with measurement data at Re=40000, showing a good correspondence. The results of the computations show that the flow with higher Reynolds number has a shorter reattachment length. By increasing the Reynolds number, the number of horseshoe vortex in the upstream decreases. The flow field structure in the upstream was almost similar for both the time-averaged and the instantaneous. But on the downstream, it did not show any similarity and had a complex flow field structure.

Stresses fluctuated and became strongly negative within the recirculation region and more strongly positive at the reattachment points. As the Reynolds number increases, the number of horseshoe vortex decreases. Therefore, it can be concluded that the maximum value of $u'v'$ only occurs at the sides of the cube.

REFERENCES

1. Castro, I. P. and Robins, A. G., "The Flow Around Surface-Mounted Cube in Uniform and Turbulent Streams", *Journal of Fluid Mechanics*, **34(7)**, PP 307-335(1977).
2. Castro, I. P., J., "Measurements in Shear Layers Separating From Surface-Mounted Bluff Bodies", *Journal of Wind Engineering and Industrial Aerodynamics*, **7**, PP 253-272(1981).
3. Schofield, W. and Logan, E., "Turbulent Shear Flow Over Surface-Mounted Obstacles", *ASME Journal of Fluids Engineering*, **112**, PP 376-385(1990).
4. Larousse, A., Martinuzzi, R., and Tropea, C., "Flow Around Surface-Mounted, Three-Dimensional Obstacles", 9th International Sym. on Turbulent Shear Flow, Springer-Verlag, PP 127-139(1991).
5. Martinuzzi, R. and Tropea, C., "The Flow Around Surface-Mounted Prismatic Obstacles Placed in A Fully Developed Channel Flow", *ASME Journal of Fluids Engineering*, **115**, PP 85-92(1993).
6. Hussein, H. J. and Martinuzzi, R. J., "Energy Balance for Turbulent Flow Around A Surface Mounted Cube Placed in A Channel", *Physics of Fluids*, **8**, PP 764-780(1996).
7. Shah, K. B. and Ferziger, J. H., "A Fluid Mechanicians View of Wind Eengineering: Large Eddy Simulation of Flow Past A Cubic Obstacle", *Journal of Wind Engineering and Industrial Aerodynamics*, **67&68**, PP 211-224(1997).
8. Rodi, W., Ferziger, J. H., Breuer, M. and Pourquie M., "", Workshop on LES of Flows Past Bluff Bodies, Rotach-Egern, Germany, (1995).
9. Krajnovic, S., and Davidson, L., "Large Eddy Simulation of The Flow Around A Bluff Body", *AIAA Journal*, **40(5)**, PP 927-936(2002).
10. Krajnovic, S., and Davidson, L., "A Mixed One-Equation Subgrid Model for Large-Eddy Simulation", *International Journal of Heat and Fluid Flow*, **23**, PP 413-425(2002).
11. Rahnama, M., and Farhadi, M., "Large Eddy Simulation of Flow Over A Wall-Mounted Cube", Proceeding of 12th Annual Conference of Computational Fluid Dynamics, Ottawa, Canada, PP 708-714(2004).
12. Rahnama, M., and Farhadi, M., "Large Eddy Simulation of Separated Flow over a Wall-Mounted Cube", Accepted to Published in International Journal of Science and Technology, (2006).
13. Hwang, J. Y., and Yang, K. S., "Numerical Study of Vortical Structures Around A Wall-Mounted Cubic Obstacle in Channel Flow", *Physics of Fluids*, **16(7)**, PP 2382-2394(2004).
14. Metais, O., and Lesieur, M., "Spectral Large Eddy Simulations of Isotropic and Stably-Startified Turbulence", *Journal of Fluid Mechanics*, **239**, PP 157-194(1992).
15. Lesieur, M., and Metais, O., "New Trends in LES of Turbulence", *Annual Review of Fluid Mechanics*, **28**, PP 45-82(1996).
16. Ferziger, J. H., and Peric, M., *Computational Methods for Fluid Dynamics*, 2ndEd., PP 273(1996).
17. Keylocka, C. J., Hardyb, T. R. J., Parsonsc, D. R., Fergusonb, R. I., Laneb, S. N., and Richardsd, K. S., "The Theoretical Foundations and Potential for Large-Eddy Simulation (LES) in Fluvial Geomorphic and Sedimentological Research", *Earth-Science Reviews*, **71**, PP 271-304(2005).